Development of a control strategy for efficient operation of a CSTR reactor

Dana Copot[1], Clara Ionescu[1], Andres Hernandez[1], Joris Thybaut[2] and Robin De Keyser[1]
[1]Department of Electrical energy, Systems and Automation, Ghent University
Technologiepark 914, B9052, Ghent-Zwijnaarde, Belgium
[2]Department of Chemical Engineering, Ghent University
Technologiepark 914, B9052, Ghent-Zwijnaarde, Belgium
Email: {Dana.Copot, ClaraMihaela.Ionescu, Andres.Hernandez, Jorys.Thybaut, Robain.DeKeyser}@UGent.be

***Abstract*—This paper describes the development of a suitable control strategy for the heating process of a lab-scale continuous stirred tank reactor (CSTR) is presented. Influence of the operational conditions, such as propeller speed, preheating the inlet gases and catalyst basket are analyzed. The study objectives in this paper are twofold: first, a control strategy for bringing the reactor at the operating point as fast as possible and second, a control strategy which is able to keep the system within specified temperatures interval. The results obtained indicate that the control strategies developed for the lab-scale CSTR reactor have good performance and the objectives were successfully achieved.**

***Index Terms*—identification, internal model control, CSTR reactor**

I. Introduction

In chemical industry, continuous stirred tank reactors (CSTR) represent the main compartment of many plants [1], [2], [3]. From the system engineering point of view, CSTR belong to a class of nonlinear systems where both steady state and dynamic behavior are nonlinear [4]. Nowadays, control design engineering has claimed considerable attention in the field of chemical industry [2], [5], [6], [7], [8]. A maximum efficiency of a chemical process with respect to product quality, production rate and operating cost, can only be achieved via an accurate control of the operating conditions which, e.g. in case of highly exothermic reactions, is not an evident matter [3], [5], [7]. Particular chemical processes show a highly non-linear behavior with respect to temperature and therefore advanced control strategy is required. Development of new control techniques remains a growing field of interest, and provides a means to tackle issues as described above [3], [5], [6], [7], [8].

Control of chemical reactors is a challenging task and therefore is one of the most interesting research areas from the point of view of process control [9], [10]. Extensive research on reactor control has been done and pioneering work such as [1], [11], [12] has provided a solid contribution to the researchers who followed. In such chemical processes the key controlled variable is temperature (which is also the focus of this research). Temperature could be named as the ”dominant variable” for control while ensuring a stable and effective operation. Small variations in temperature would cause significant changes with respect to the dynamics of the reaction. A representation of typical elements in a CSTR reactor is shown in figure 1.

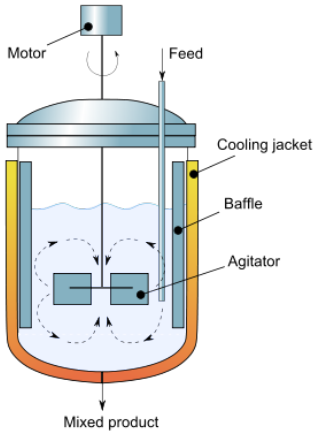

Fig. 1. Schematic representation of a CSTR reactor.

The focus of this paper is to design a suitable control strategy for a lab-scale CSTR reactor. The maximum work temperature of the reactor is 800 K and a pressure up to 5MPa is allowed. For an uniform heat distribution, the reactor is provided with a magnetically driven propeller with a maximum speed of 2500 rpm.

From the control point of view the following objectives have to be achieved. First, to reduce as much as possible the necessary time required by the reactor to reach the operating point (this is called *Induction phase*). Second, a control strategy has to be developed in order to keep the system stable once the operating point is being reached (this is called *Maintenance phase*).

The structure of the paper is as follows: In *Section 2* a detailed description of the system is presented followed by *Section 3* where identification is performed. In *Section 4* the control strategies for induction and maintenance phase are presented. In *Section 5* the results obtained on the real set-up are discussed.

978-1-4799-8481-7/15/$31.00 ©2015 IEEE

II. System description

The reactor used in this research is a lab-scale CSTR used for kinetic data acquisition of gas-solid reactions at high pressures and temperatures. The reactor is essentially a hollow stainless steel cylinder with an internal volume of about 1.45 10^{-3} m^3. Sealing is provided by an aluminium ring placed in between the two flanges. Heating of the reactor is provided via heating of three resistors placed in a thermal cap with a total power of 3000 W. The upper two heating elements (800 and 1100 W) are grouped in one input signal, $U1$, while the lower resistor (1100 W) is represented by $U2$. A schematic representation of the heat flow into the system is given in figure 2.

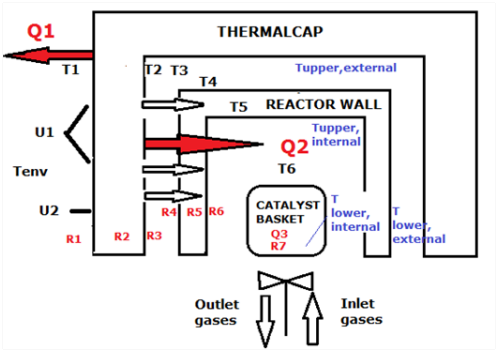

Fig. 2. Schematic overview of the heating mechanism of the Berty reactor.

In figure 2 Q1, Q2 and Q3 represent the heat dissipated to respectively the environment, the reactor and the catalyst basket. U1 and U2 represent the heat sources, R1 to R6 thermal resistances and T1 to T6 the local temperatures. For control purposes only internal lower and internal upper temperatures are measured, while $U1$ and $U2$ are manipulated.

A thick insulation layer inside the thermal cap ensures an almost adiabatic behavior of the system. The bottom of the reactor is placed on a thick insulation layer and no heat losses are considered in the lower part of the reactor.

Heat transfer towards the internal part of the Berty reactor is a very slow process due to the inert mass of the reactor and the numerous heat transfer resistances between the thermal cap and the internal thermocouples. The external upper and external lower temperatures, i.e., the temperature at the outside surface of the reactor and, hence, approximately the temperature of the thermal resistors, rise up immediately after applying a voltage to the thermal cap while the increase in internal temperature is significantly delayed. This highlights that the internal temperatures exhibit a slower dynamics than the external temperatures.

A direct consequence of the slow system dynamics is a large difference between the internal and external temperatures during the induction phase. The difference between the internal and the external part of the reactor is preferably maintained in a specified interval in order to avoid failure of the aluminium seal. Leaking implies the release of flammable gases such as hydrogen, and possible contact of the catalyst with surrounding oxygen resulting in degeneration or deactivation. If this constraint is satisfied, then the settling time for star-up is about 10 hours.

The heating rate of the reactor depends on factors such as: the propeller speed, preheating of the inlet gas flow and catalyst basket. The impact of these factors on the temperature profile is discussed below.

Influence of the propeller speed: the role of the propeller is to provide a homogeneous temperature profile inside the reactor. A higher speed implies a more effective distribution of the heat and the gases. In Table 1, the external and internal temperatures measured after one hour of operation at different propeller speeds are shown. A higher speed apparently implies a faster heating of the reactor and a reduced discrepancy between both internal temperatures. A propeller speed of 1250 rpm, which corresponds to 50% of its maximum capacity has been selected for experiments. This value has been chosen in order to avoid excessive wear of the propeller carbon bearings.

Propeller speed (rpm)	T_{extLow}	T_{extUp}	T_{intLow}	T_{intUp}
500	618	543	425	484
1000	601	554	435	484
1250	640	605	462	506

TABLE I
TEMPERATURE VALUES (K) AT DIFFERENT PROPELLER SPEED DURING ONE HOUR OF OPERATION AT MAXIMUM POWER INPUT (OPEN CATALYST BASKET, GASES NOT PREHEATED, 100% POWER APPLIED)

Influence of the catalyst basket: the geometry of the catalyst basket (see figure 3) also exhibits a considerable effect on the internal temperature profiles. A closed geometry involves a larger inert mass to heat up, but also more heat that is transferred through conduction. However, in this case the open catalyst basket geometry will be used due to its most frequent application in kinetic data acquisition.

Fig. 3. Catalyst basket geometry (left: closed; right: open).

Influence of the preheating of the inlet gases: theoretically, preheating the inlet gases should result in a faster heating of the reactor. The temperature profile acquired from an experiment in which hydrogen entered the reactor unheated was compared with the profile where the gases were heated up to 200 ^{o}C prior to reaction. The results suggested that preheating of the inlet gases had only a negligible effect on the internal temperature as only minor differences were observed between both profiles. The low heat capacity of hydrogen and its bad functioning as a heat transfer medium may explain these observations.

III. Identification for Control

The operating temperature for the internal part of the reactor is chosen at 250 ^{o}C which represents a typical reaction temperature for alkane hydrocracking. The settling time is minimized by applying maximum power, i.e. 3000 W during the induction phase, on both $U1$ and $U2$, in each experiment. After approximately one hour, the heating elements are turned off in order to allow the temperatures to settle around the operating point.

To avoid complex modeling (i.e. to complete these equations information about the external insulation of reactor is needed, this information is not available at this moment), black box parametric identification has been considered. The dynamics of the heating process can be described using two input and four output variables (figure 4 left): the inputs are the two voltages applied to the $U1$ and $U2$, and the outputs are the four temperatures upper and lower internal temperatures and upper and lower external temperatures.

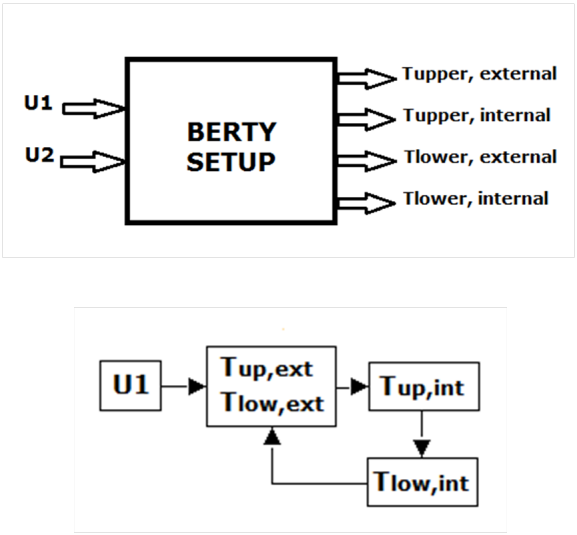

Fig. 4. Top: Input-output scheme of the Berty reactor. Bottom: Schematic representation of temperatures flow.

Process identification is based on obtaining a transfer function (TF) which accurately describes the process behavior. We will consider the input-output behavior of $U1$ and the upper internal temperature only. The input $U1$ comprises the upper two resistors with a combined power of 1900 W and has a direct influence on the external upper temperature profile. The latter affects directly the internal upper temperature profile which, in turn, determines the dynamics of the internal lower temperature.

Several experiments were performed in order to understand how the heat is transferred from the external to the internal part, and how the interactions occur within the reactor.

For the purposes of control, due to the significantly different dynamics of the system, two different identifications were performed: i) the TF representing the transient to reach the set-point (i.e. induction phase) and ii) the TF characterizing the dynamics of the process around the operating point (i.e.

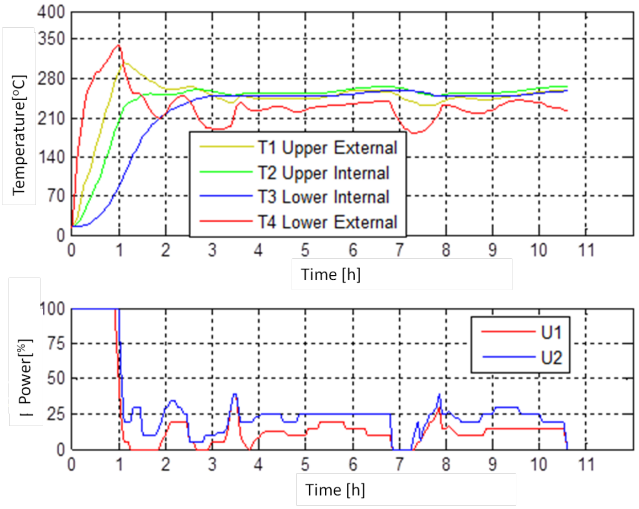

Fig. 5. Induction and maintenance phase in the temperature profile of the Berty setup.

maintenance phase) Temperatures profiles in the reactor are shown. In figure 5 for both induction and maintenance. After 7 hours, the inputs $U1$ and $U2$ go to zero. The lower external temperature present an interesting behavior, decreasing much faster than upper external temperature. This means that $U2$ presents faster dynamics towards the lower external temperature compared to $U1$ towards the upper external temperature.

For induction phase several experiments were performed in order to find the optimal values for the inputs. The experiment with the following specifications for $U1$ and $U2$ was performed for identification purposes: during the first 50 minutes of the experiment both $U1$ and $U2$ were set at 100% in order to increase the temperature very fast and reach the set-point as soon as possible. After 50 minutes $U1$ was set on 0% and $U2$

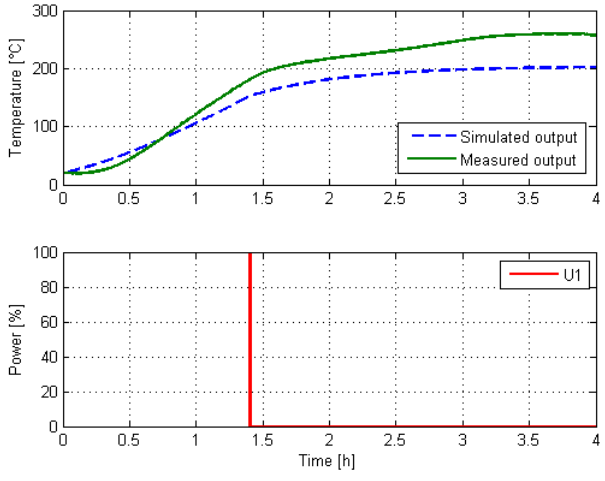

Fig. 6. Simulation results obtained using the identified transfer function (1) for induction phase.

was set at 30%. The response is depicted in figure 6. It can be noticed that near the set-point, there is significant difference between the simulated and measured data. This difference is due to the nonlinearities of the system at higher temperatures. From this experiment we can take the conclusion that the set-point can be reached in approximately 2 hours. Using this data the following transfer function has been obtained:

$$H(s) = \frac{13.68610^{-4}(s + 10.0710^{-}3)}{s(s + 37.8710^{-4})} \quad (1)$$

Therefore, to achieve the goal for the induction phase (i.e. reaching the operating point as fast as possible) this is not taken into consideration.

Once the operating point is reached, we initiate data collection for the maintenance phase. The specifications for $U1$ and $U2$ are as following: during the first 20 minutes $U1$ was set at 100%, the next 160 minutes $U1$ was set at 0, followed by another 15 minutes at 100% power. During the entire experiment for maintenance phase $U2$ was kept constant at 30%. The identified transfer function for maintenance phase has the form presented in (2).

$$H(s) = \frac{-61.810^{-5}(s - 4.810^{-}3)}{(s + 73.310^{-4})(s + 11.110^{-6})} \quad (2)$$

The result obtained for this protocol is depicted in figure 7.

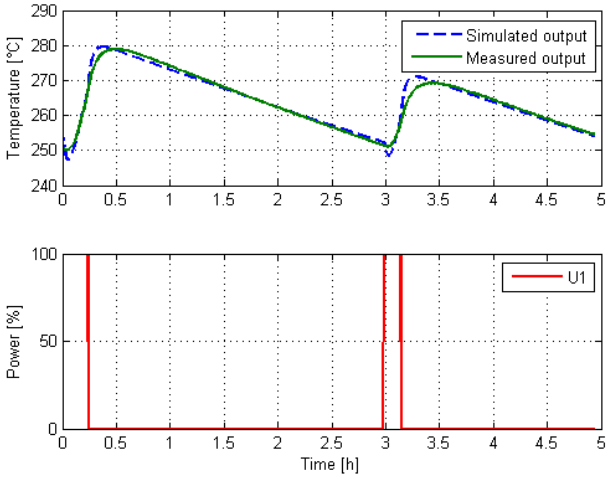

Fig. 7. Simulation results obtained using the identified transfer function (2) for maintenance phase.

IV. Control Strategies

For induction phase a P controller for $U1$ with the following specifications: settling time - 4 hours, overshoot - 10% and robustness - 70% has been designed. The controller has been tuned using the FRTool toolbox [13]. The controller has been applied to the real system and the results are depicted in figure 8. The upper graph shows the temperature profile and the lower graph shows the control effort. The set-point has been reached in approximatively 2 hours, fulfilling also the condition that around the operating point the difference between the internal upper and internal lower temperature do not exceed 20^oC. Therefore, we can conclude that the first challenge (i.e. reaching the operating point as fast as possible) has been successfully performed.

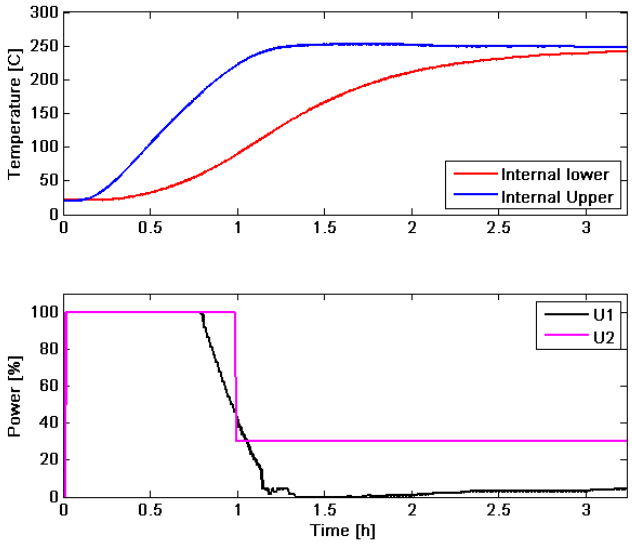

Fig. 8. Results obtained with the P controller for the induction phase on the real Berty CSTR plant.

Now that the first goal has been fulfilled, a control strategy for the second objective is being developed. The aim of this controller is to keep the system stable during reactions. For this, a model based control strategy will be considered, i.e. internal model control (IMC) [14], [15].

The IMC is a model-based controller which relies on the use of the internal plant model [15], [16]. The IMC controller performance is dependent on how well the model approximates the actual process. An IMC closed loop control scheme is depicted in figure 9, where $\frac{B(q^{-1})}{A(q^{-1})}$ is the system PTF (Pulse Transfer Function), the discrete-time equivalent of the process transfer function. $F(q^{-1})$ is a filter which ensures a proper compensator and represents the desired closed loop performance. In the IMC context, the controller is designed based on compensating the process dynamics while ensuring desired closed loop performance.

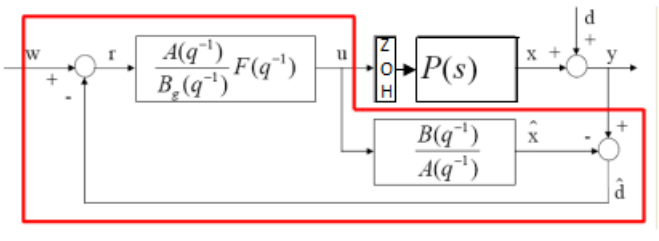

Fig. 9. Schematic overview of the IMC closed loop control scheme.

Split the process transfer function $\frac{B(q^{-1})}{A(q^{-1})}$ in an invertible

(good) part and a non-invertible (bad) part. This implies that if the transfer function has time delays or zeros outside the unit circle of z-plane, they are thus part of the non-invertible (bad) part of the process, denoted as $B_b(q^{-1})$; with the normalization $B_b(1) = 1$. The remaining invertible (good) part of the process is then denoted by:

$$\frac{B_g(q^{-1})}{A(q^{-1})} \tag{3}$$

A 'basic' IMC filter, designed to follow step changes in the setpoint and to reject step disturbances at the output of the process, is given by:

$$F(q^{-1}) = \frac{(1+a)^n}{(1+a\cdot q^{-1})^n} \tag{4}$$

with steady state gain $F(1) = 1$ and a a design parameter defined as

$$a = -e^{-T_s/\lambda} \tag{5}$$

The values of this design parameter are in the range $0 << |a| < 1$ and it is related to the closed-loop speed: if λ is big, the $|a|$ is closer to 1, making the controller less aggressive, with a higher settling time. The case of the extended filter is not described in this paper, but elsewhere [14].

The discrete-time IMC controller $R(q^{-1})$ can be represented into an equivalent closed loop control scheme as depicted in figure 10.

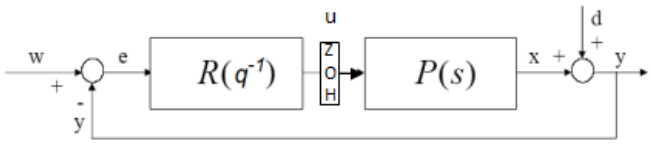

Fig. 10. Equivalent Discrete-IMC representation for $R(q^{-1})$.

We can now describe the IMC controller as an equivalent $R(q^{-1})$ with structure given by:

$$R(q^{-1}) = \frac{A(q^{-1})F(q^{-1})}{B_g(q^{-1}) - B(q^{-1})F(q^{-1})} \tag{6}$$

Based on the identified transfer function for the maintenance phase the IMC controller has been designed. The discretized transfer function of the process (2), with a sampling time of 10 min, has the following form:

$$H(z) = \frac{0.1049z + 0.1341}{z^2 - 1.006z + 0.0122} \tag{7}$$

Once the set-point is reached with the P controller it is necessary to switch to the IMC controller which will maintain the system within the desired interval. The IMC control strategy has been tested on the real plant, using $\lambda = 1000$ seconds and $n = 3$. The closed loop control obtained results obtained on the real system are presented in figure 11. During this experiment two set-point changes were performed. From these results we can conclude that the IMC control strategy has good performance during the maintenance phase, i.e. lower internal temperature follows the profile of the upper internal temperature within a 20^oC difference.

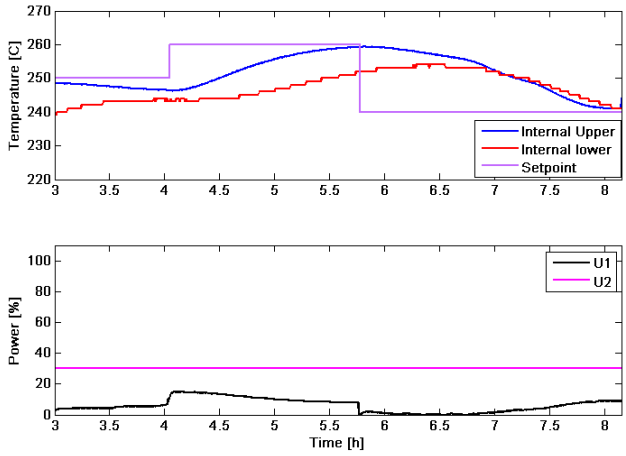

Fig. 11. IMC controller performance for the maintenance phase on the real Berty CSTR plant.

V. Discussion and Conclusions

In this paper, the development of a control strategy for the heating process of a lab-scale setup was elaborated aiming at a low settling time. Two dynamic phases in the temperature profile are distinguished: induction and maintenance. The induction phase compromises the regime during which the reactor is heating up to the operating point. The maintenance phase is when the reactor operates in steady state. The effect of specific reactor conditions, such as the propeller speed, preheating of the inlet gases, and catalyst basket on the internal temperature profile has been studied.

Two control strategies were designed and tested on the real system. The main goal has been achieved, i.e. a decrease of the settling time was possible during the induction phase. Also for the maintenance phase the IMC controller gives satisfactory results. The performance achieved with the induction control strategy gives good results and a reduction the settling time has been obtained. The temperature upper internal reaches the set-point (i.e. 250 ^{o}C) in approximatively 2 hours. At the beginning both powers ($U1$ and $U2$) were set at 100% in order to increase the temperature as fast as possible. After 1 hour $U2$ is set at 30% and is kept at this values for the rest of the closed loop experiment.

The motivation for designing two different controller (induction and maintenance) is that for the induction we need to reach the set-point as fast as possible while in maintenance it is necessary to have a robust controller which can cope with disturbances that can occur during reactions. Therefore a P controller for the induction phase is sufficient to achieve our goal, while for the maintenance phase a model based control strategy is needed.

REFERENCES

[1] Aris, R., Amundson, N.R. An analysis of chemical reactor stability and control. Chemical Engineering Science, 7, 1958.

[2] Stephanopoulos G., Chemical Process Control. An Introduction to theory and Practice. Prentice Hall international Series in the physical and chemical engineering sciences, 2004.

[3] Bequette B.W., Process Control: Modeling, Design and Simulation, Prentice Hall India, 2008.

[4] Piovoso M.J., Kosanovich K. A., Rokhlenko V., Guez A., Nonlinear Adaptive Control with Parameter Estimation of a CSTR, Journal of Process Control, 5(3), 137-148, 1995.

[5] Z.F. Zuhwar, The Control of Non Isothermal CSTR Using Different Controller Strategies, Iraqi Journal of Chemical and Petroleum Engineering, 13(3), 35-45, 2012.

[6] D. Krishnaa, K. Suryanarayanab, G. Aparnab, and R. Padma Sree, Tuning of PID Controllers for Unstable Continuous Stirred Tank Reactors, International Journal of Applied Science and Engineering, 10(1), 1-18, 2012.

[7] R. Kommineni, IMC Based PID Controller Design for a Jacketed CSTR, Proc. of the Intl. Conf. on Advances in Computer, Electronics and Electrical Engineering, doi:10.3850/978-981-07-1847-3 P0575, 2012.

[8] P. Negi, Frequency domain analysis of Optimal Tuned IMC- PID Controller for Continuous Stirred Tank Reactor (CSTR), International Journal of Electronics, Electrical and Computational System, 2(1), 2014.

[9] Bhat A., Chidambaram M., Madhavan K.P., Nonlinear Feedback Control of a CSTR, Chemical Engineering Communications , 101(1), 1991.

[10] J. Lee, J. Lee, Progress and Challenges in Control of Chemical Processes. Annual Review of Chemical and Biomolecular Engineering, 5, 383-404, 2014.

[11] Foss A.S., Chemical reaction system dynamics. Chemical Engineering Progress, 54(9), 1959.

[12] Perlmutter D.D., Stability of Chemical Reactors; Prentice Hall: New York, 1972.

[13] R. De Keyser, C. Ionescu, FRtool: A frequency response tool for CACSD in Matlab, IEEE Conference on Computer Aided Control Systems Design, 2006.

[14] R. De Keyser, C. Copot, A. Hernandez, C.Ionescu, Discrete-time internam model control with disturbance and vibration rejection. accepted for publication in Journal of Vibration and control, 2015.

[15] Morari M., Rivera D.E., Skogestad S., Internal model control: PID controller design, 25(1), 252-265, 1986.

[16] J. Garrido, F. Vzquez, F. Morilla, Inverted decoupling internal model control for square stable multivariable time delay systems. Journal of Process Control 24, 1710-1719, 2014.